PCCP

Nuclear quantum and H/D isotope effects on aromaticity: path integral molecular dynamics study

Journal:	*Physical Chemistry Chemical Physics*
Manuscript ID	CP-ART-03-2024-001331.R2
Article Type:	Paper
Date Submitted by the Author:	24-Jun-2024
Complete List of Authors:	Udagawa, Taro; Gifu University Faculty of Engineering Graduate School of Engineering, Tanaka, Hikaru; Gifu University Kuwahata, Kazuaki; Yokohama-city University, Graduate School of Nanobioscience Tachikawa, Masanori; Yokohama-city University, Graduate School of Nanobioscience

Data availability statements

The data supporting this article are included as part of the Supplementary Information.

ARTICLE

Nuclear quantum and H/D isotope effects on aromaticity: path integral molecular dynamics study

Hikaru Tanaka,[a] Kazuaki Kuwahata, [b] Masanori Tachikawa [b] and Taro Udagawa *[a]

Received 00th January 20xx,
Accepted 00th January 20xx

DOI: 10.1039/x0xx00000x

Aromaticity is an important concept in organic chemistry, and thus, many theoretical and experimental studies have been conducted so far. However, the majority of theoretical studies have concentrated on the aromaticity of the stationary point structures. Herein, the influence of nuclear quantum fluctuation (nuclear quantum effects: NQEs) and thermal fluctuation on the aromaticity of benzene have been analyzed by path integral molecular dynamics (PIMD) simulation. The PIMD simulations revealed that the NQEs affected not only the C-H bonds but also the C-C bonds. The HOMA and NICS calculations demonstrated that the aromaticity decreased due to the NQEs of carbon atoms, attributed to an increase in the contribution from specific vibrational modes strongly correlated with benzene's aromaticity.

Introduction

Aromaticity is a distinctive property observed in cyclic and planar molecules with 4n + 2 (n = 0, 1, 2…) π electrons.[1] The delocalized π electrons stabilize the energy and induce equalization of the bond lengths. Even though the aromaticity is a very important concept, it is defined in various ways.[2–5] Thus, there are several methods for assessing the degree of aromaticity. Theoretical calculations have been used for a long time to evaluate the degree of the aromaticity. The harmonic oscillator model of aromaticity (HOMA)[6] and the nucleus-independent chemical shifts (NICS)[7] are the representative theoretical methods to evaluate the molecular aromaticity. The HOMA estimates the aromaticity based on bond lengths, whereas the NICS estimates the aromaticity based on its response to an external magnetic field. These indices have been widely used to assess the aromaticity of various molecules and ring fragments so far.[8–10]

It is known that molecules fluctuate at any temperature. Nevertheless, most theoretical studies evaluated the aromaticity only for optimized structures. Hence, the effects of thermal fluctuation on the aromaticity were not considered in such studies. Although aromatic rings tend to become flat and are considered rigid, recent theoretical studies have revealed that even the C_6-ring framework of benzene is not rigid but highly flexible. [11–13] Thus, several groups have analyzed the aromaticity of molecule, taking thermal fluctuations into account with molecular dynamics (MD) simulations. Cysewski suggested that structural distortions arising from the normal mode may have an impact on the delocalization of π electrons in benzene, even at room temperature.[14] Dopieralski studied the deuterium isotope effect (H/D isotope effect) on the molecular structure and the aromaticity of furan using ab initio MD simulation.[15] These studies demonstrated that thermal fluctuations are important in assessing molecular aromaticity. However, fluctuations arising from the quantum nature of nuclei (nuclear quantum effect: NQE) were rarely taken into account in previous theoretical studies.[16–18] In conventional quantum chemistry calculations, nuclei are not treated quantum mechanically because they are much heavier than electrons. Therefore, the NQEs have been ignored. However, it is known that NQEs often become important for light nuclei, such as proton and deuteron. For example, several groups and we have reported that NQEs of hydrogen nuclei enhance the hydrogen bond strength and facilitate proton transfer reactions.[19–24] Furthermore, we have also demonstrated that considering the NQEs is indispensable for the analysis of the H/D isotope effects. [24]

The NQEs of heavier atoms, such as carbon, have not been focused because their nuclei are much heavier than electrons. However, several recent studies have pointed out that the NQEs are also important when calculating the electronic structures of carbon atoms.[25,26] Kundu et al. performed the ab initio path integral MD (PIMD) simulations in combination with a quantum thermostat.[26] They found that the NQEs have a substantial impact on the electronic properties of amorphous carbon. They advocated that the NQEs are also significant in even carbon atom to determine the electronic structure.

---

[a] Department of Chemistry and Biomolecular Science, Faculty of Engineering, Gifu University, Yanagido 1-1, Gifu 501-1193, Japan.
E-mail: udagawa.taro.f1@f.gifu-u.ac.jp.
[b] Graduate School of NanobioScience, Yokohama City University, 22-2 Seto, Kanazawa-ku, Yokohama 236-0027, Japan.

† Electronic Supplementary Information (ESI) available: See DOI: 10.1039/x0xx00000x

From the above, it can be inferred that the NQEs should be considered in order to analyze the aromaticity accurately. However, to the best of our knowledge, there are no theoretical studies that have analyzed aromaticity with considering the NQEs so far. Thus, we would like to investigate the NQEs on aromaticity in this study. The simplest aromatic molecule, benzene, was chosen as the focus of this study. Additionally, we also investigate the H/D isotope effects on the aromaticity by analyzing deuterated benzene.

Computational Detail

First, we determined the level of electronic structure calculation for the PIMD simulations. The C-H and C-C bond lengths in the equilibrium structure of benzene obtained by CCSD(T)/aug-cc-pVQZ method were 1.0830 Å and 1.3954 Å, respectively. Note that since benzene has D6h symmetry, all six C-H bond lengths are exactly equal, and similarly, all six C-C bond lengths are exactly equal. Since PIMD simulations require a very large number of atomic force calculations, it is essential to select an appropriate calculation level that can reproduce the results obtained by a highly accurate method at a low computational cost. We found that the APFD/6-311G[27] level of calculation can reproduce the CCSD(T)/aug-cc-pVQZ geometry well. The C-H and C-C bond lengths obtained by APFD/6-311G calculation were 1.083 Å and 1.396 Å, respectively. We also confirmed that the APFD/6-311G calculation adequately reproduced the normal modes (NMs) of benzene obtained from the CCSD(T)/aug-cc-pVQZ calculation. The NMs are listed in Table S1 of the SI. Thus, APFD/6-311G was adopted for the PIMD simulations. In addition, the "int(grid=finegrid)" keyword implemented in Gaussian16 was utilized to reduce the computational cost.

In this study, we performed PIMD simulations on benzene (C_6H_6) and deuterated benzene (C_6D_6). In the PIMD simulations, all nuclei were treated as quantum particles, and each nucleus was expanded using 16 beads. We have confirmed that $P = 16$ is sufficient for the present study by preliminary PIMD simulations (see Figure S1 in the Supplementary information). *On-the-fly* ab initio PIMD simulations were performed for 90,000 steps after 10,000 steps of thermal equilibration run, with a timestep size of 0.1 fs. The Classical molecular dynamics (CLMD) simulation, in which each nucleus was represented by only one bead and hence the NQEs were not considered, was also carried out for benzene for 400,000 steps, after 100,000 steps of thermal equilibration run. Both the PIMD and CLMD simulations were conducted in the canonical ensemble (NVT) at 300 K. Moreover, we used the massive Nosé-Hoover chain thermostats[28,29] with the chain length parameter $L = 4$, combined with the velocity Verlet algorithm for efficient sampling. The PIMD simulations were performed using a house code.[30,31]

The HOMA and NICS methods were employed to evaluate the aromaticity of benzene. The HOMA evaluates the aromaticity in terms of bond lengths.[6] The HOMA value is calculated by the following equation:

$$\mathrm{HOMA} = 1 - \frac{257.7}{n}\sum_i^n \left(d_{opt} - d_i\right)^2 \quad (1)$$

where n is the number of C-C bonds, d_{opt} is the optimized bond length of the reference molecule (1.388 Å), and d_{i} is the i's C-C bond length obtained by each simulation. In addition, 257.7 is the normalization constant. According to the definition of the HOMA scheme, aromaticity of a molecule is evaluated as the sum of the squared deviations of the C-C bond lengths from those in the ideal aromatic molecule: HOMA = 1 indicates that the target molecule is a perfectly aromatic, while HOMA = 0 indicates a non-aromatic character. For example, the HOMA value is 0.997 for the optimized structure of benzene calculated at APFD/6-311G level.

The NICS index[7] is calculated based on a magnetic shielding constant estimated at the center of the target ring (NICS(0)). Negative (positive) NICS values indicate that the target ring is aromatic (anti-aromatic), respectively. The NICS value is often evaluated at 1.0 Å above the ring center (NICS(1)) to prevent contamination of the contribution from π electrons. In addition, the zz component of the NICS(1) value, denoted as NICS(1)zz, is also commonly used for analyses. These NICS values (NICS(1) and NICS(1)zz) are generally considered better aromaticity indices compared to NICS(0).[3] It should be noted here that the benzene does not strictly maintain its planarity during the simulation. Hence, the NICS(0) value was evaluated at the center of gravity of the six carbon atoms of benzene. In addition, we defined the least-squares plane for the six carbon atoms of benzene to measure NICS(1) and NICS(1)zz. The NICS(1) values were evaluated at 1.0 Å above and below the center of gravity in the least-squares plane.

Results and Discussion

Nuclear quantum effects for structural parameters

Figure 1 shows the one-dimensional distribution of C-H and C-C bond lengths obtained by PIMD(H), PIMD(D), and CLMD simulations.

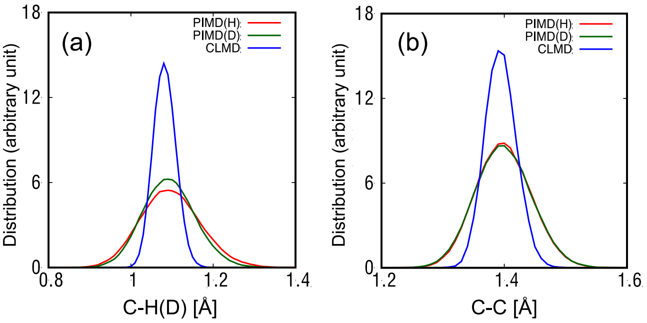

Figure 1. One-dimensional distributions of (a) C-H bond lengths and (b) C-C bond lengths obtained by PIMD and CLMD simulations.

First, we examined the one-dimensional distributions of C-H bond lengths as depicted Figure 1(a). In a comparison of the PIMD(H), PIMD(D), and CLMD results, we discovered that the PIMD(H) and PIMD(D) distributions were broader than the CLMD distribution due to the nuclear quantum fluctuations.

Furthermore, it is noteworthy that the PIMD(H) distribution is slightly broader than that of PIMD(D). This disparity (H/D isotope effects) can be attributed to the differences in nuclear quantum nature of proton and deuteron, arising from the difference in the masses of proton and deuteron. This difference affects the stretching motion of the C-H/C-D bond. Next, we focused on the distribution of C-C bond lengths illustrated in Figure 1(b). Similar to the C-H bond lengths, the distributions of PIMD(H) and PIMD(D) were broader than that of CLMD. However, unlike C-H bond lengths, the distribution of PIMD(H) and PIMD(D) were nearly identical. Therefore, the difference between CLMD and PIMD distributions was attributed to the NQEs of carbon nuclei themselves, not the secondary NQEs of the hydrogen nuclei. These results demonstrate that even the NQEs of heavy atoms can sometimes directly influence the bond lengths.

Nuclear quantum effects on aromaticity

The HOMA values were calculated at every snapshot structure obtained from each simulation. The distribution of the HOMA values was illustrated in Figure 2, and the average HOMA values for each simulation were listed in Table 1.

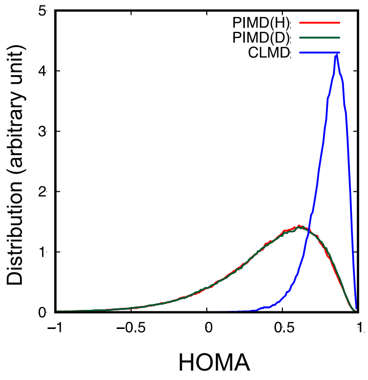

Figure 2. One-dimensional distributions of HOMA values obtained in PIMD(H) (red), PIMD(D) (green), and CLMD (blue) simulations.

Table 1. Average HOMA value obtained in PIMD and CLMD simulations and HOMA value at the equilibrium structure (EQ).

	PIMD(H)	PIMD(D)	CLMD	EQ
HOMA	0.418	0.419	0.804	0.997

In the CLMD distribution, the HOMA values were primarily distributed within a narrow range between 0.5 and 1, and the average value of CLMD (0.804) did not become significantly smaller compared to the EQ value. This fact suggests that the decrease in the aromaticity of benzene due to thermal effects is not so significant. The HOMA values for PIMD(H) and PIMD(D) were distributed to a lower range than the CLMD. In other words, the aromaticity was clearly reduced due to the NQEs. On the other hand, the results of PIMD(H) and PIMD(D) were nearly identical for both the distributions and the average values. This tendency is consistent with the distributions of C-C bond lengths (Figure 1), in which the NQEs of hydrogen nuclei had no significant effects on the C-C bond lengths constituting the benzene ring.

HOMA is a simple index that evaluates aromaticity solely based on C-C bond lengths. Details of the electronic structure, such as polarization effects, were not considered in the calculated HOMA values. To gain a deeper insight into the aromaticity, we also calculated NICS values for every snapshot structure. The distributions of NICS values obtained from each simulation were shown in Figure 3. Additionally, Table II lists the average NICS values obtained in each simulation.

Table 2. Average NICS value (ppm) obtained in PIMD and CLMD simulations and NICS value at the equilibrium structure (EQ).

	PIMD(H)	PIMD(D)	CLMD	EQ
NICS(0)	-6.85	-6.87	-7.03	-7.26
NICS(1)	-10.39	-10.43	-10.64	-10.79
NICS(1)zz	-25.45	-25.54	-26.17	-26.53

The one-dimensional distribution of NICS values obtained by CLMD simulation distributed within a narrow range around the EQ value, as shown in Figure 3. The average NICS values of CLMD were slightly larger than those of EQ, but smaller than those of PIMD. The distribution of NICS values obtained in PIMD simulations was distributed over a wider range than in the CLMD simulation. In addition, unlike the HOMA results, PIMD(H) and PIMD(D) distributions were slightly different, and the average values of PIMD(H) and PIMD(D) were also not identical. In other words, the NICS results might suggest the

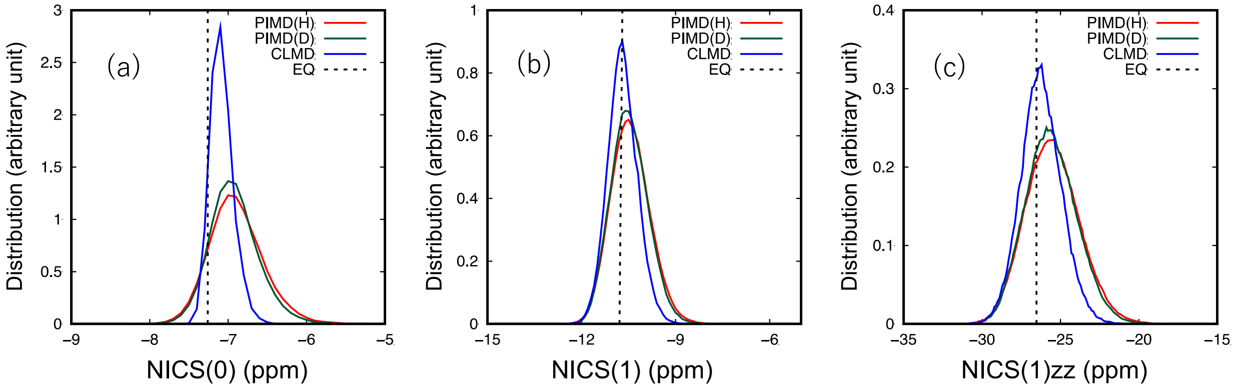

Figure 3. One-dimensional distributions of (a) NICS(0) (b) NICS(1), and (c) NICS(1)zz.

existence of a modest H/D isotope effect on the aromaticity, unlike the HOMA results.

Normal mode analysis and contribution ratio of each vibration mode

In order to identify the factor contributing to the reduction of the aromaticity due to the NQEs, firstly, we performed normal mode analysis to examine the changes in aromaticity resulting from variations according to each normal vibrational mode of benzene. We can specify which NM(s) provides a significant impact on aromaticity from this analysis. By identifying the important vibrational mode(s), we can gain insights into the underlying mechanisms responsible for the observed changes.

Benzene possesses 30 NMs, however, some of them are degenerate due to D_{6h} symmetry. Consequently, benzene has 20 unique NMs. The lowest vibrational mode was calculated to be 421.24 cm^{-1}, which corresponds to 606 K, at the APFD/6-311G level. Therefore, we do not need to consider the vibrational excited state in the present analysis because the PIMD and CLMD simulations have been performed at 300 K. Figure 4 illustrates the changes in NICS(1)zz for each NM up to the classical turning point, which corresponds to the approximate maximum amplitude in the NM motion (see, Supplementary Information). Figure 4 provides information about the influence of individual NMs on the aromaticity of benzene.

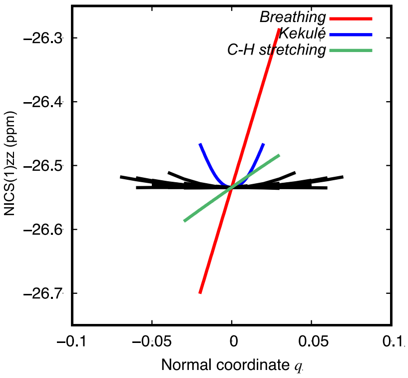

Figure 4. NICS(1)zz values along normal coordinate q. Red, blue, and green lines represent the changes in NICS(1)zz values according to structural distortions induced by *Breathing*, *Kekulé* and *C-H stretching* vibrational modes, respectively. Black lines represent the changes induced by other vibrational modes.

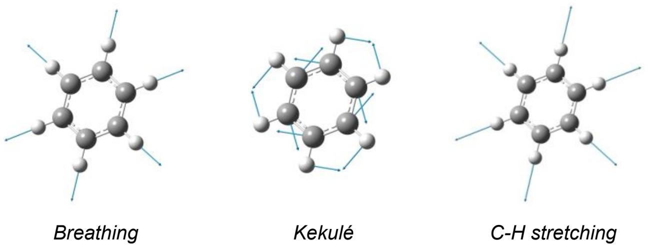
Breathing *Kekulé* *C-H stretching*

Figure 5. Three NMs strongly correlated with the aromaticity of benzene. The names are given arbitrarily.

Obviously, three NMs (named *Breathing* (1019.28 cm^{-1}), *Kekulé* (1364.65 cm^{-1}), and *C-H stretching* (3220.63 cm^{-1}), illustrated in Figure 5), have significant effects on the aromaticity. Breathing mode induces expansion and contraction of the entire benzene ring, whereas *Kekulé* vibrational mode leads D_{6h} benzene to D_{3h} (*Kekulé*) benzene structure. In addition, *C-H stretching* corresponds to the *C-H stretching* vibrational mode. *Breathing* and *C-H stretching* decrease aromaticity during ring expansion and raise it during contraction, *Kekulé* vibration, on the other hand, always decrease aromaticity. As shown in Figure 5, these three modes were categorized into in-plane mode. On the other hand, other NMs were found to contribute less to the aromaticity. In addition, some previous studies also pointed out that aromaticity was sensitive to in-plane vibrations.[14] Therefore, these in-plane vibrational modes may strongly influence the aromaticity of benzene.

We then calculated the inner product of the NM vectors and the displacement vector defined by the difference between each snapshot structure and the equilibrium structure. This analysis allows us to assess the contribution ratio of each NM to the snapshot structure. In the present study, we calculated the inner product for only the aforementioned three vibrational modes.

Figure 6 showed the one-dimensional distributions of the inner product of the NM vectors and the vectors defined by the difference between each snapshot structure and the

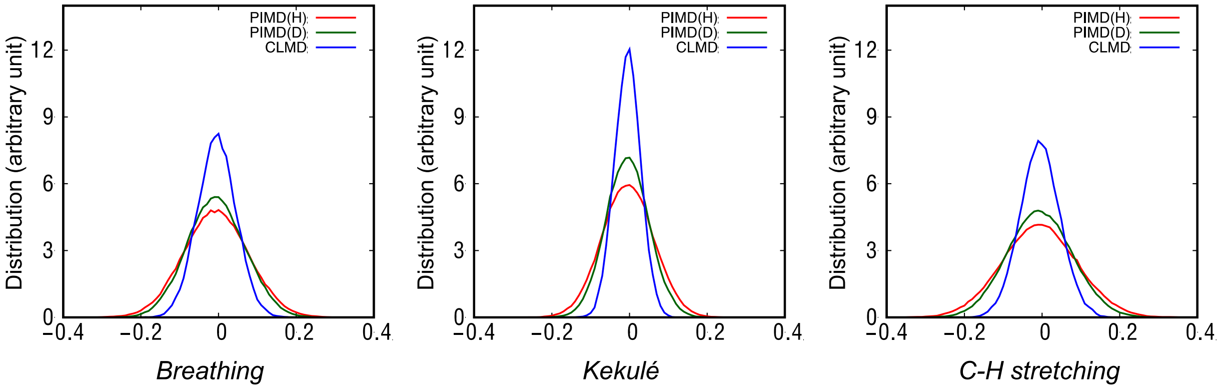

Breathing *Kekulé* *C-H stretching*

Figure 6. One-dimensional distributions of the inner product of the vector defined by the difference between each snapshot structure and the equilibrium structure and the NM vectors.

equilibrium structure. Thus, the distributions represented the magnitude of the contributions from the *Breathing*, *Kekulé*, and *C-H stretching* vibrational modes, and appear to be almost symmetrically spread over the positive and negative ranges centered on 0. Broader distributions were obtained by the PIMD simulation, indicating that the NQEs expanded the width of the distribution.

However, since positive variations along *Breathing* and *C-H stretching* modes increase NICS value, while negative variations decrease it, the NQEs on these modes do not induce any H/D isotope effects on the average NICS value. Only the variations along the *Kekulé* mode affect the NICS average value; these variations reduced aromaticity. This is why only modest H/D isotope effects were observed in the average NICS values.

Therefore, we revealed that while the NQEs influenced the magnitude of the contributions from each vibrational mode, they resulted in only slight effects on aromaticity.

Conclusions

In this study, we investigated the NQEs and H/D isotope effects on benzene and deuterated benzene to analyze the effect of the quantum nature of nuclei on aromaticity using ab initio PIMD method and CLMD.

Considering the NQEs, we observed the increase in fluctuations not only in the C-H bond lengths but also in the C-C bond lengths, indicating that even the NQEs of carbon atoms cannot be ignored. The HOMA index, which estimates the aromaticity based on bond lengths, and NICS index, which estimates the aromaticity reflecting the electronic states, showed a decrease in aromaticity due to the NQEs. The NICS results revealed that the aromaticity of benzene might be slightly reduced by deuterium substitution due to the increase in the contribution from the *Kekulé* vibrational mode. We found that the NQEs of not only light nuclei, such as hydrogen nuclei, but also heavier atoms' nuclei affected chemical properties such as aromaticity. Therefore, it is crucial to consider the NQEs of all atoms for a comprehensive understanding of chemical properties.

Author Contributions

T.U. designed the study and the main conceptual ideas. H.T. performed the PIMD simulations. H.T. and T.U. conducted the analysis for the PIMD results. All authors aided in interpreting the results and worked on the manuscript. T.U. and M.T. supervised the project. All authors have given approval to the final version of the manuscript.

Conflicts of interest

There are no conflicts to declare.

Acknowledgements

The present study was supported by JSPS KAKENHI Grant Nos. 21K04991 and 22H02141 (to T.U.), Nos. 22KJ2564 and 23K13827 (to K.K.), and Nos. 21H00026 and 23K17905 (to M.T.). The generous allotment of computational time from the Research Center for Computational Science, Okazaki, Japan (Project No: 23-IMS-C256 to T.U.), is also gratefully acknowledged. This work was financially supported by JST SPRING, Grant Number JPMJSP2125. H.T. would like to take this opportunity to thank the "Interdisciplinary Frontier Next-Generation Researcher Program of the Tokai Higher Education and Research System".

Notes and references

1 E. Hückel, ***Z. Phys.***, 1931, **70**, 204–286.
2 L. Pauling, and J. Sherman, ***J. Chem. Phys.***, 1933, **1(8)**, 606–617.
3 H. J. Dauben, J. D. W. Jr., and J. L. Laity, ***J. Am. Chem. Soc.***, 1968, **90**, 811–813.
4 Y. B. Guo, Z. Z. Liu, H. X. Liu, F. Y. Zhang, and J. Q. Yin, ***Spectrochim.***, 2016, **Acta A**, 84–88.
5 H. Szatylowicz, P. A. Wieczorkiewicz, and T. M. Krygowski, ***Sci***, 2022, **4(2)**, 24.
6 T. M. Krygowski, M. K. Cyrañski, Z. Czarnocki, G. Häfelinger, and A. R. Katritzky, ***Tetrahedron***, 2000, **56**, 1783–1796.
7 P. Von, R. Schleyer, C. Maerker, A. Dransfeld, H. Jiao, N. J. R. Van, and E. Hommes, ***J. Am. Chem. Soc.***, 1996, **118**, 6317–6318.
8 F. Feixas, E. Matito, J. Poater, and M. Solà, ***J. Phys. Chem. A***, 2007, **111(20)**, 4513–4521.
9 G. Berionni, J. I. C. Wu, and P. v. R. Schleyer, ***Org. Lett.***, 2014, **16(23)**, 6116–6119.
10 M. Zilka, S. Sturniolo, S. P. Brown, and J. R. Yates, ***J. Chem. Phys.***, 2017, **147,** 144203.
11 O. V. Shishkin, P. Dopieralski, I. V. Omelchenko, L. Gorb, Z. Latajka, and J. Leszczynski, ***J. Phys. Chem. Lett.***, 2011, **2(22)**, 2881–2884.
12 Ł. Walewski, P. Dopieralski, O. V. Shishkin, and Z. Latajka, ***Int. J. Quantum Chem.***, 2014, **114**, 534–542.
13 T. Udagawa, H. Tanaka, T. Hirano, K. Kuwahata, M. Tachikawa, M. Baba, and U. Nagashima, ***J. Phys. Chem. A***, 2023, **127(4)**, 894–901.
14 P. Cysewski, ***Phys. Chem. Chem. Phys.***, 2011, **13(28)**, 12998–13008.
15 P. Dopieralski, I. V. Omelchenko, and Z. Latajka, ***Molecules***, 2021, **26**, 2889.
16 M. E. Tuckerman, D. Marx, M. L. Klein, and M. Parrinello, ***Science***, 1997, **275(5301)**, 817–820.
17 C. Schran, F. Brieuc, and D. Marx, ***J. Chem. Phys.***, 2021, **154**, 051101.
18 K. Kuwahata, S. Ito, and M. Tachikawa, ***J. Chem. Phys.***, 2023, **159**, 104301.
19 M. Ceriotti, J. Cuny, M. Parrinello, and D. E. Manolopoulos, ***Proc. Natl. Acad. Sci.*** 2013, **110**, 15591.
20 M. Ceriotti, W. Fang, P.G. Kusalik, R.H. McKenzie, A. Michaelides, M. A. Morales, and T. E. Markland, ***Chem. Rev.*** 2016, **116**, 13, 7529.
21 C. Ngaojampa, T. Kawatsu, Y. Oba, N. Kungwan, and M. Tachikawa, ***Theor. Chem. Acc.***, 2017, **136**, 30.
22 K. Sugiura, M. Tachikawa, and T. Udagawa, ***RSC Adv***., 2018, **8(31)**, 17191-17201.
23 H. Tanaka, K. Kuwahata, M. Tachikawa, and T. Udagawa, ***ACS Omega***, 2022, **7(16)**, 14244–14251.

24 T. Udagawa, H. Yabushita, H. Tanaka, K. Kuwahata, and M. Tachikawa, ***Phys. Chem. Chem. Phys***., 2023, **25(23**), 15798-15806.

25 A. Kundu, M. Govoni, H. Yang, M. Ceriotti, F. Gygi, and G. Galli, ***Phys. Rev. Mater.***, 2021, **5(7)**, L070801.

26 A. Kundu, Y. Song, and G. Galli, ***Proc. Natl. Acad. Sci. U.S.A.***, 2022, **119(31)**, e2203083119.

27 A. Austin, G. A. Petersson, M. J. Frisch, F. J. Dobek, G. Scalmani, and K. Throssell, ***J. Chem. Theory Comput.***, 2012, **8(12)**, 4989–5007.

28 M. E. Tuckerman, D. Marx, M. L. Klein, and M. Parrinello, ***J. Chem. Phys.***, 1996, 104, 5579–5588.

29 G. J. Martyna, M. E. Tuckerman, D. J. Tobias, and M. L. Klein, ***Mol. Phys.*** 1996, 87, 1117.

30 M. Shiga, M. Tachikawa, and S. Miura, ***Chem. Phys. Lett.***, 2000. **332**, 396.

31 M. Shiga, M. Tachikawa, and S. Miura, ***J. Chem. Phys.***, 2001, **115**, 9149.

32 H. Fallah-Bagher-Shaidaei, C. S. Wannere, C. Corminboeuf, R. Puchta, and P. v. R. Schleyer, ***Org. Lett.***, 2006, **8(5)**, 863–866.